Electronic Supplemental Information (ESI)

A top-down synthesis of wurtzite Cu_2SnS_3 nanocrystals for efficient photoelectrochemical performance

Weijun Sun, Yangwei Ye, Yu You and Jun Xu*

School of Electronic Science & Applied Physics, Micro Electromechanical System Research Center of Engineering and Technology of Anhui Province, Hefei University of Technology, Hefei, 230009, P.R. China

* E-mail: apjunxu@hfut.edu.cn

Experimental Section

Synthesis of Cu_2O nanocubes. Cu_2O nanocubes were synthesized by reacting an ascorbic acid aqueous solution with an $[Cu(OH)_4]^{2-}$ complex solution at room temperature, which was described in detail in our previous report.[1]

Synthesis of wurtzite Cu_2SnS_3 nanoboxes and nanocrystals. 10 mL of $SnCl_4 \cdot 5H_2O$ aqueous solution (0.0375 M) was dropwise added into 20 mL of $Na_2S \cdot 9H_2O$ aqueous solution (0.375 M) to form a transparent tin chalcogenide complex (Sn-MCC) solution. Then, 20 mL of the Cu_2O nanocubes aqueous suspension (0.0375 M) was added to the above Sn-MCC solution under magnetic stirring. An HCl solution was added into the mixed solution, where the pH value was adjusted to near neutral (~7.5). Afterwards, the mixed suspension was transferred into a Teflon-lined stainless steel autoclave, which was sealed and kept at 190 °C for designed durations, i.e., 1 h for the wurtzite Cu_2SnS_3 nanoboxes and 20 h for the wurtzite Cu_2SnS_3 nanocrystals. The black products were collected and washed with distilled water and absolute ethanol several times. Furthermore, tetragonal Cu_2SnS_3 can be obtained by annealing the as-prepared wurtzite Cu_2SnS_3 nanostructures in argon at 430 °C for 30 min.

Growth of ZnO nanorod arrays on FTO substrates. Arrays of ZnO nanorods on FTO glass substrates were synthesized by a seed-assistant hydrothermal method, which has been described in our previous reports.[2,3]

Preparation of various ZnO/Cu_2SnS_3 electrodes. The as-prepared wurtzite Cu_2SnS_3 nanocrystal (or nanobox) ink with a concentration of ~5 mg/mL were coated on the ZnO nanorod arrays by a spin-coating technique. After annealing at 430 °C for 30 min

in argon, tetragonal Cu_2SnS_3 nanocrystals modified ZnO nanorod array was obtained.

Characterization. Morphologies, sizes, crystal structures, compositions and optical properties of the various samples were studied with X-ray diffraction (XRD, Rigaku D/Max 2500v diffractometer, Cu Kα radiation), scanning electron microscopy (SEM, Philips XL30 FEG), transmission electron microscopy (TEM, JEOL JEM-2100F, 200 kV), Raman spectroscopy (Lab RAM HR, 532 nm excitation), X-ray photoelectron spectroscopy (XPS) (Thermo ESCALAB 250Xi, Al Kα), and UV-vis spectroscopy (Cary 5000).

PEC measurements. A standard three-electrode configuration in a quartz cell was assembled to carry out PEC performance of the samples using an electrochemical workstation (CHI 660E). The simulated sunlight (CEAULIGHT, CEL-S500) under AM 1.5G illumination at a power density of 100 mW cm^{-2} was employed as the light source. A Pt foil and a saturated calomel electrode (SCE) were used as the counter electrode and the reference electrode, respectively. A Na_2SO_4 aqueous solution (0.5 M) was used as the electrolyte, which was degassed by bubbling pure N_2 for 30 min prior to measurements. The various ZnO/Cu_2SnS_3 electrodes on the FTO glass substrates with an active area of 0.2 cm^2 were used as the photoanodes for PEC water splitting. Linear sweep voltammetry (LSV) was carried out at an scan rate of 5 mV s^{-1} for the polarization curves. The potentials were carefully calibrated to a normal hydrogen electrode (NHE).

Table S1 Recent advance of the synthesis of Cu_2SnS_3 nanocrystals.

No.	Materials and morphology	Solvent	Reaction temperature and duration	References
1	Cu_2SnS_3 quantum dots	Ethylene glycol	180 °C, 12 h	Inorg. Chem., 2017, 56, 2198–2203
2	Cu_2SnS_3 quantum dots	DDT	230 °C, 50 min	RSC Adv., 2017, **7**, 23301–23308
3	Cu_2SnS_3 nanocrystals	Oleylamine	160 °C, 30 min	Chem. Mater., 2015, 27, 1342−1348
4	Cu_2SnS_3 nanocrystals	Oleylamine	240 °C, 20 min	CrystEngComm, 2014, 16, 8642–8645
5	Cu_2SnS_3 nanocrystals	ODE	140 °C, 30 min	CrystEngComm, 2016, 18, 2885–2893
6	Cu_2SnS_3 nanocrystals	ODE	220 °C, 12 h	CrystEngComm, 2013, 15, 5612–5619
7	Cu_2SnS_3 nanorods	Oleylamine	290 °C, 10 min	Chem. Commun., 2015, 51, 13810–13813
8	Cu_2SnS_3 nanocrystals	Deionized water	190 °C, 20 h	This work

Table S2 Recent advance of the Cu-based electrodes for PEC application.

No.	Photoelectrode	Electrolyte	Applied Potential (V)	Photocurrent Density (mA cm^{-2})	Stability	References
1	$ZnO/CuInS_2$	Na_2S (1 M)	0.29 (vs. SCE)	17.5	/	Int. J. Hydrogen Energy, 2012, 37, 15029–15037.
2	$TiO_2/CuInS_2$	KOH (1 M)	0.74 (vs. Ag/AgCl)	19.07	No decay, 5 min	Phys. Chem. Chem. Phys., 2014, 16, 16204–16213.
3	Pt/ALD-TiO_2/CdS/CZTS	Na_2SO_4 (0.5 M)	-2 (vs. RHE)	13	75%, 60 min	ACS Energy Lett., 2016, 1, 1127−1136.
4	CZTS/Zn(O,S)/TiO_2	Na_2SO_4 (0.5 M)	1.23 (vs. NHE)	15.05	67%, 60 min	J. Mater. Chem. A, 2017, 5, 4695–4709.
5	TiO_2/Zn(O,S)/CZTS	Na_2SO_4 (1 M)	1.23 (vs. RHE)	8.84	80%, 120 min	ACS Catal. 2017, **7**, 8077−8089.
6	ZnO/CZTSSe	Na_2SO_4 (0.5 M)	1.23 (vs. NHE)	9.06	65%, 60 min	J. Mater. Chem. A, 2017, 5, 25230–25236.
7	CZTS/FTO	$Eu(NO_3)_3$ (0.2 M)	0.5 (vs. Ag/AgCl)	1.8	No decay, 6 min	Chem. Commun., 2011, 47, 3141–3143.
8	ZnO/Cu_2SnS_3	Na_2SO_4 (0.1 M)	0.5 (vs. SCE)	0.46	No decay, 4 min	RSC Adv., 2016, 6, 104041–104048.
9	$CuRhO_2$	NaOH (1 M)	-0.9 (vs. SCE)	1.08	43%, 8 h	J. Am. Chem. Soc., 2014, 136, 830−833.
10	ZnO/t-Cu_2SnS_3	Na_2SO_4 (0.5 M)	1.23 (vs. NHE)	6.46	73%, 60 min	This work

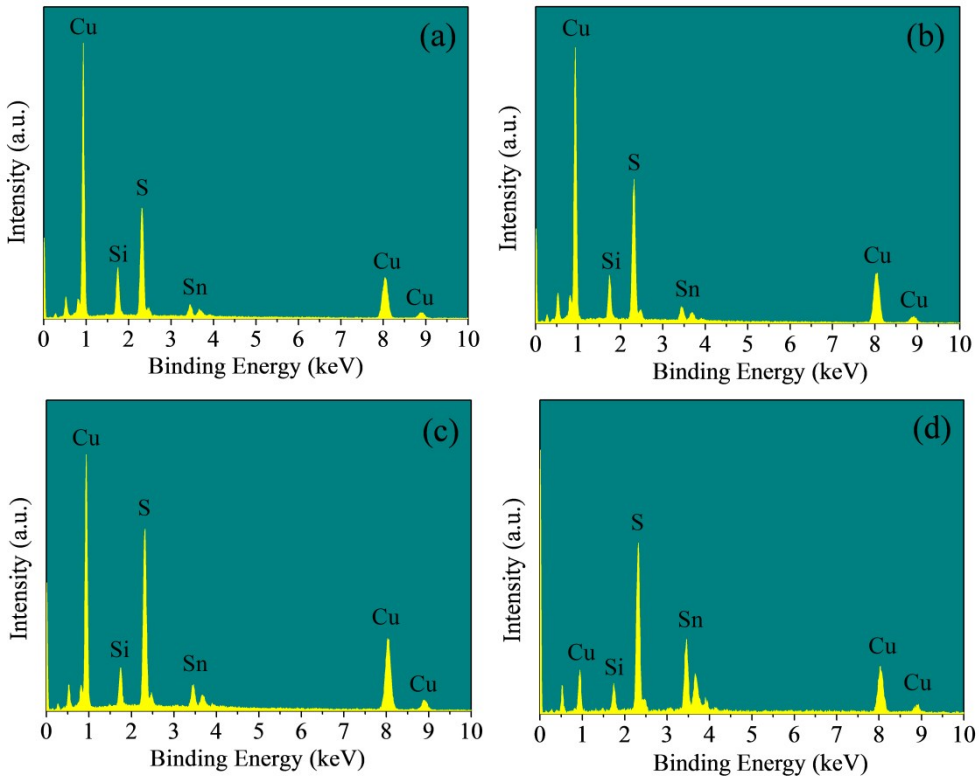

Fig. S1 EDX spectra of (a) the Cu_7S_4 nanoboxes, (b) the CuS nanoboxes obtained after hydrothermal reaction for 20 min, (c) the CuS nanoboxes obtained after hydrothermal reaction for 40 min, (d) the Cu_2SnS_3 nanoboxes obtained after hydrothermal reaction for 1 h. These samples were coated on Si wafers for EDX measurement.

It is observed that very slight Sn contents (1-4 at%) were detected for the Cu_7S_4, CuS (20 min) and CuS (40 min) nanoboxes (Fig. S1a-c). Such a phenomenon is attributed to the adsorption of some Sn ions from the growth solution by Sn-S bonding on the surface of the various copper sulfides nanoboxes. After 1 h of hydrothermal reaction, an obvious increase in Sn content (17 at%) along with a distinct decrease in Cu content of the nanoboxes are observed (Fig. R1d), owing to the formation of Cu_2SnS_3.

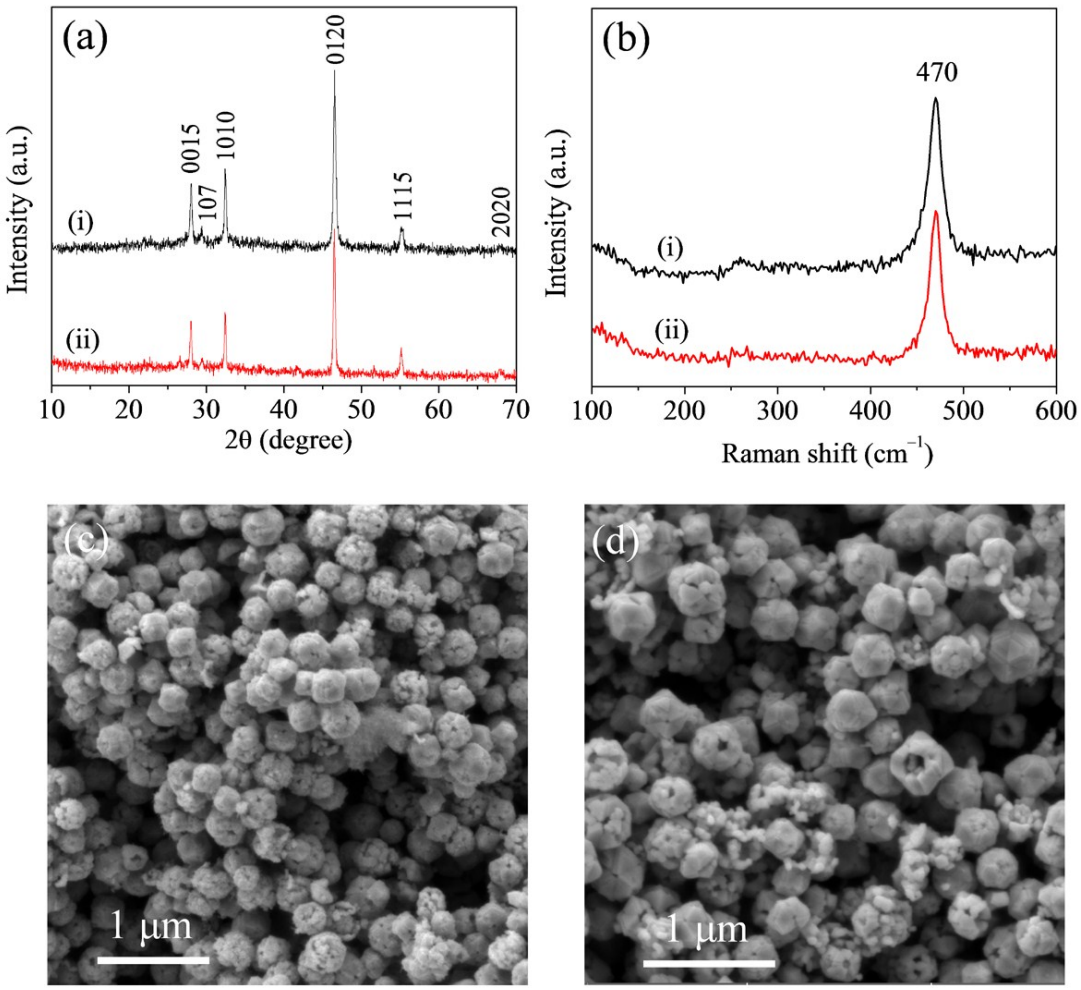

Fig. S2 (a,b) XRD patterns (a) and Raman spectra (b) of the $Cu_{1.8}S$ samples prepared in the alkaline growth solution for (i) 3 h and (ii) 20 h. (c,d) SEM images of the $Cu_{1.8}S$ sample prepared in alkaline growth solution for (c) 3 h and (d) 20 h.

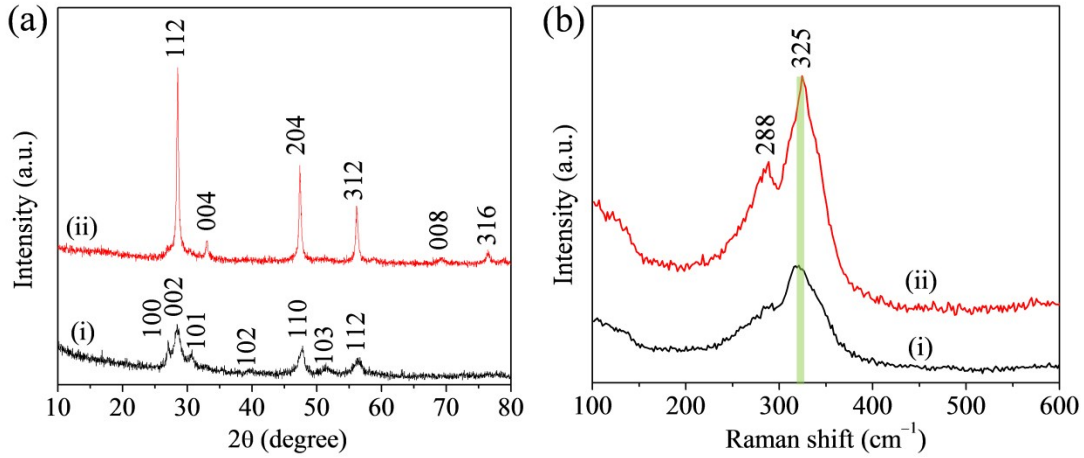

Fig. S3 XRD patterns (a) and Raman spectra (b) of the wurtzite Cu_2SnS_3 nanocrystals before (i) and after (ii) post-thermal annealing at 430 °C in a N_2 flow.

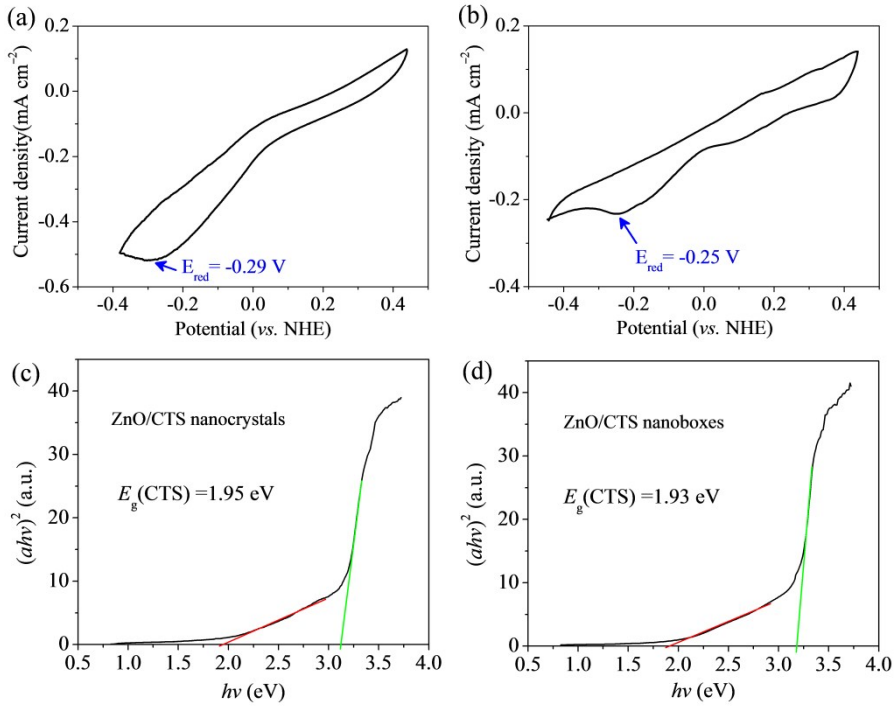

Fig. S4 (a,b) CV curves of (a) the w-CTS nanocrystals and (b) the w-CTS nanoboxes at 10 mV s^{-1}. (c,d) the dependence of $(ahv)^2$ on hv for the ZnO/w-CTS-NC and the ZnO/w-CTS-NB.

The band levels of the CTS nanoboxes and nanocrystals can be determined by the electrochemical cyclic voltammetry (CV) method. The CTS electrodes, a Pt foil, and a calomel electrode were used as the working electrode, the counter electrode and the reference electrode, respectively. The CV curves were presented in **Fig. S4a and S4b**. The reduction peaks in the cyclic volammograms correspond to the conduction band (CB) positions. It is revealed that E_{red} is -0.29 V (vs. NHE) for the CTS nanocrystals and -0.25 V (vs. NHE) for the CTS nanoboxes.

The CB energy level value can be calculated according to the following relation (ACS Appl. Mater. Interfaces 2017, 9, 34915−34926; J. Phys. Chem. A 2004, 108, 376−383):

$E_{CB} = eE_{red}$ (V) = -4.5 (eV) – e E_{red} (*vs*. NHE) (1)

Thus, the E_{CB} value is calculated to be -4.21 eV for the w-CTS nanocrystals and -4.25 eV for the w-CTS nanoboxes.

The bandgap (E_g) of the can be calculated by UV-vis absorption spectra shown in Fig. 4c in the manuscript. It is revealed that the bandgap is estimated to be 1.95 eV for the

w-CTS the nanocrystals and 1.93 eV for the w-CTS the nanoboxes (Fig. S4c and S4d). ZnO has a bandgap of 3.2 eV and a E_{CB} of -4.36 eV (*Proc. Natl. Acad. Sci. USA*.2011, *108*, 29). Therefore, the photoanode exhibits a type-II energy level alignment between ZnO and Cu_2SnS_3 (both nanoboxes and nanocrystals) as depicted in Fig. 4e of the manuscript.

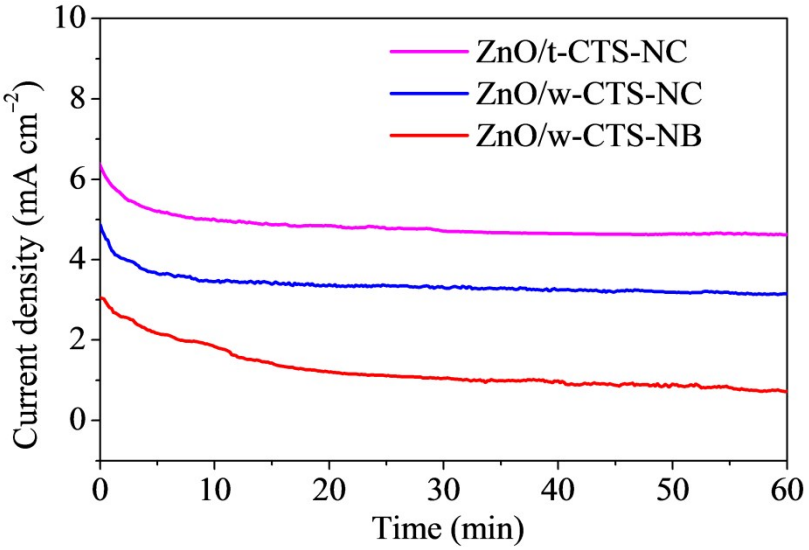

Fig. S5 Time-dependent photoresponses of the three photoanodes at a bias of 1.23 V (*vs*. NHE).

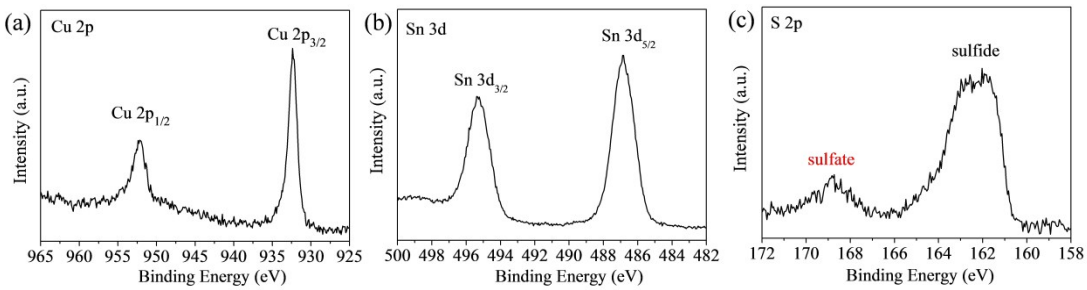

Fig. S6 XPS spectra of the ZnO/CTS photoanode after stability test. It is revealed that sulfide (S^{2-}) was partially oxidized to sulfate (SO_4^{2-}).

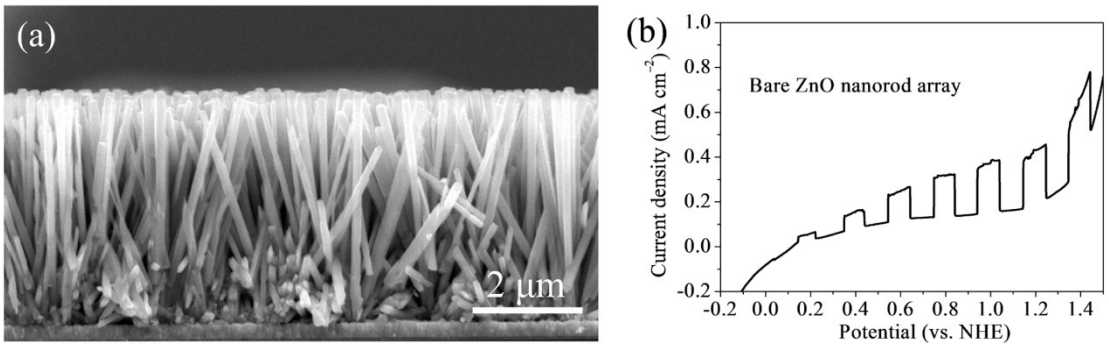

Fig. S7 (a) The SEM image of the bare ZnO nanorod array, (b) the chopped LSV curve of the bare ZnO nanorod array.

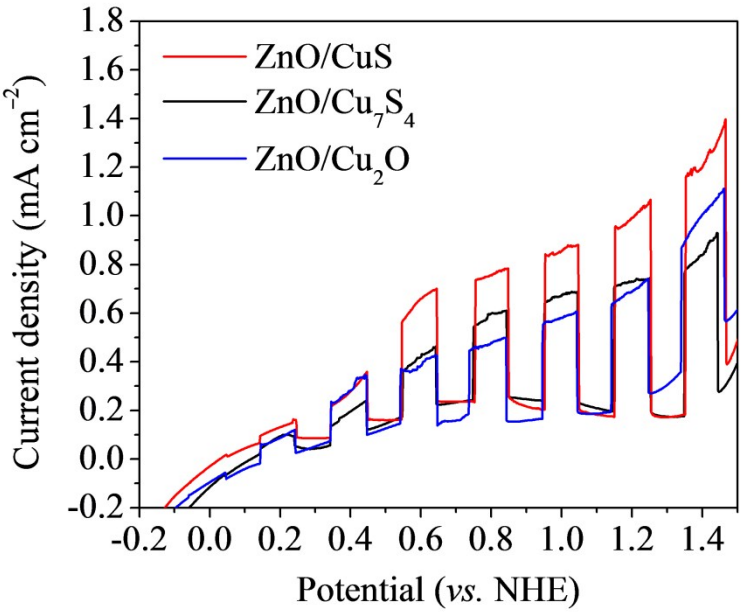

Fig. S8 The chopped LSV curves of the ZnO/Cu_2O, ZnO/Cu_7S_4 and ZnO/CuS photoanodes.

Fig. S8 shows the chopped LSV curves of the ZnO/Cu_2O, the ZnO/Cu_7S_4 and the ZnO/CuS photoanodes. It is observed that the photocurrent density at 1.23 V vs. NHE is 0.71 mA cm^{-2} for the ZnO/Cu_2O, 0.74 mA cm^{-2} for the ZnO/Cu_7S_4, 1.04 mA cm^{-2} for the ZnO/CuS. All these values are much smaller than those of the ZnO/CTS photoanodes (Fig. 4e). The poor PEC performance of the ZnO/Cu_2O photoanode is probably attributed to the weak stability of Cu_2O that is very susceptible to oxidation in solution. It is observed that the yellow Cu_2O can quickly turn to be brownish black (CuO) during PEC measurement. On the other hand, the indirect bandgap nature of Cu_7S_4 and CuS may determine their weak PEC performance relative to the ZnO/CTS photoanodes.

References:

[1] Z. Hu, R. Zhou, W. Sun, J. Zhang, C.-S. Lee and J. Xu, *Mater. Today Energy*, 2017, **5**, 331–337.

[2] J. Xu, X. Yang, Q.-D. Yang, T.-L. Wong, S.-T. Lee, W.-J. Zhang and C.-S. Lee, *J. Mater. Chem.*, 2012, **22**, 13374–13379.

[3] J. Xu, X. Yang, H. Wang, X. Chen, C. Luan, Z. Xu, Z. Lu, V. A. L. Roy, W. Zhang and C.-S. Lee, *Nano Lett.*, 2011, **11**, 4138–4143.